Original Article

iPhone-Based Cartilage Topography Scanning Yields Similar Results to Computed Tomography Scanning

Hailey P. Huddleston, M.D., Kevin Credille, M.D., M.S., Mohamad M. Alzein, B.S., William M. Cregar, M.D., Mario Hevesi, M.D., Ph.D., Nozomu Inoue, M.D., Ph.D., and Adam B. Yanke, M.D., Ph.D.

Purpose: To investigate the feasibility and accuracy of 3-dimensional (3D) iPhone scans using commercially available applications compared with computed tomography (CT) for mapping chondral surface topography of the knee. **Methods:** Ten cadaveric dysplastic trochleae, 16 patellae, and 24 distal femoral condyles (DFCs) underwent CT scans and 3D scans using 3 separate optical scanning applications on an iPhone X. The 3D surface models were compared by measuring surface-to-surface least distance distribution of overlapped models using a validated 3D-3D registration volume merge method. The absolute least mean square distances for the iPhone-generated models from each scanning application were calculated in comparison to CT models using a point-to-surface distance algorithm allowing regional "inside/outside" measurement of the absolute distance between models. **Results:** Only 1 of the 3 scanning applications created models usable for quantitative analysis. Overall, there was a median absolute least mean square distance between the usable model and CT-generated models of 0.18 mm. The trochlea group had a significantly lower median absolute least mean square distance compared with the DFC group (0.14 mm [interquartile range, 0.13-0.17] vs 0.19 mm [0.17-0.25], $P = .002$). iPhone models were smaller compared with CT models (negative signed distances) for all trochleae, 83% of DFCs, and 69% of patellae. **Conclusions:** In this study, we found minimal differences between a 3D iPhone scanning application and conventional CT scanning when analyzing surface topography. **Clinical Relevance:** Emerging 3D iPhone scanning technology can create accurate, inexpensive, real-time 3D models of the intended target. Surface topography evaluation may be useful in graft selection during surgical procedures such as osteochondral allograft transplantation.

Focal articular cartilage defects are common in the young, active patient population, with a reported prevalence of up to 66% of knees undergoing an arthroscopic procedure.[1,2] In patients with symptomatic focal chondral defects who have failed conservative measures, surgical treatment options include microfracture, autologous chondrocyte implantation, osteochondral autograft transplantation, and osteochondral allograft (OCA) transplantation.[3-7] In particular, OCA transplantation has consistently reported positive patient outcomes following an OCA procedure and 75% graft survivorship at 10 years,[8,9] but articular surface topography mismatch and incongruity after OCA transplantation increase the risk of premature OCA wear[10] and may contribute to poorer clinical outcomes.[11] As such, evaluation of chondral surface topography can improve allograft selection and minimize surface mismatch for an OCA procedure.

Currently, many graft companies rely on tibial width size measurements to select a graft donor for a recipient. Thus, one 2-dimensional measurement is being used to match 2 complex 3-dimensional (3D) surfaces. Specifically, 3D morphology such as dysplasia or radius of curvature is unlikely to be appropriately captured through a 2-dimensional measurement. Evaluation of native osseous and chondral topography can be performed with a preoperative clinical computed tomography (CT) or magnetic resonance imaging (MRI).[12] However, these techniques are mainly utilized in research settings as performing these scans for topography matching on cadaver allografts is cumbersome and expensive. Importantly, commercial allograft donor banks do not

From the Hospital for Special Surgery, New York, New York, U.S.A. (H.P.H., N.I., A.B.Y.); Houston Methodist Hospital, Houston, Texas, U.S.A. (K.C.); Department of Orthopedics, Rush University Medical Center, Chicago, Illinois, U.S.A. (M.M.A.); OrthoCarolina, Charlotte, North Carolina, U.S.A. (W.M.C.); and Mayo Clinic, Rochester, Minnesota, U.S.A. (M.H.).

Received June 19, 2023; accepted March 24, 2024.

Address correspondence to Adam B. Yanke, M.D., Ph.D., 1611 W Harrison St, St 300, Chicago IL 60612, U.S.A. E-mail: Adam.yanke@rushortho.com

2666-061X/23871

https://doi.org/10.1016/j.asmr.2024.100936

have CT or MRI scanners available, and OCAs must be harvested within 24 hours of allograft donor death to limit potential contamination.[13,14] Furthermore, while information from CT or MRI could assist preoperatively in identifying the ideal donor and graft harvest location, it would be unable to provide any intraoperative guidance if observed recipient chondral topography were to vary significantly from preoperative imaging.

Newer imaging technologies are emerging, such as augmented reality (AR) in which a 3D model is superimposed on the surgeon's view.[15,16] Practical applications of AR beneficial to orthopaedic surgery have been demonstrated mostly in multiple cadaveric and animal studies, although AR clinical studies are becoming more common. AR theoretically could provide intraoperative guidance on ideal graft harvest location during procedures such as OCA but is also limited by the need for formal preoperative CT or MRI.[15,16] Cheaper options, such as smartphone scanning, may present a more feasible solution to directing graft harvest location in procedures such as OCAs. Scanning applications available in iPhone and iPad (Apple) models have the ability to create an inexpensive real-time 3D model of an intended target surface with a quick iPhone scan with the various iPhone cameras and sensors that enable depth perception. Some scanning applications utilize the iPhone rear-facing light detection and ranging (LiDAR) sensor while others utilize the iPhone self-facing TrueDepth camera, which employs a vertical-cavity surface-emitting laser (VCSEL) technology patented by Apple.[17-19] VCSEL combines the traditional and infrared camera with a proximity sensor, dot projector, and flood illuminator to emit and sense infrared light to generate depth maps and 3D models with machine learning algorithms.[20-23]

iPhone-generated models may provide accurate cartilage topographic information in human cadaveric specimens. This approach could guide intraoperative graft selection location during an OCA procedure. However, the feasibility of these iPhone scanning applications in comparison to traditional CT scans remains unknown. Therefore, the purpose of this study was to investigate the feasibility and accuracy of 3D iPhone scans using commercially available applications compared with CT for mapping chondral surface topography of the knee. We hypothesize that 3D models created by commercial iPhone applications will have minimal differences when compared with CT scan models.

Methods

This study was exempt from institutional review board approval due to the use of deidentified specimens. The specimens were donated from a large tissue bank (AlloSource). All specimens did not have any osteochondral pathologies, such as osteoarthritis or chondromalacia. Specimens were macroscopically confirmed for absence of chondral defects and osteoarthritis. If substantial chondral defects and/or osteoarthritis was present, the specimen would be excluded. The senior author (A.B.Y.) evaluated each specimen for dysplasia and included ones with signs of dysplasia for use in this study. Based on this, a total of 24 distal femoral condyles (DFCs), 16 patellae, and 10 trochleae were included in analysis.

iPhone Scan and CT Data Acquisition and Processing

The cadaveric specimens underwent CT (BrightSpeed; GE Healthcare) scanning with a standard protocol (120 kV, slice thickness of 0.625 mm, 512 × 512 matrix). The CT images were exported as DICOM files and segmented with a threshold level of −500 HU to create articular and bone surface models using commercially available segmentation software (v.22 Research; Materialise Mimics). The 3D scans were acquired with an iPhone X (Apple). For each specimen, 3 surface scans were performed using 3 commercially available applications: Qlone (EyeCue Vision Technologies), Trnio (Trnio) and Scandy (Scandy). All 3 applications scanned through different approaches. Qlone and Trnio used the iPhone's rear-facing LiDAR sensor.[17-19] Qlone required printing a square mat that was composed of small black and white squares. After printing the pattern onto paper, the specimen was placed in the center. To scan, the user had to slowly circularly walk around the specimen and scan it at different heights, maintaining that the iPhone was perpendicular to the articular surface being scanned. Trnio involved a similar approach but did not require the printed mat. When scanning at regular intervals, Trnio would acquire an image. The images were then automatically combined within the application to generate the final surface model. In contrast, Scandy used the iPhone's self-facing TrueDepth VCSEL technology-based camera, which features 7-megapixel resolution.[17-19] For Scandy, the iPhone was slowly moved and rotated around the object to obtain the final surface model. Once the scan was acquired, the surface models were exported directly as an STL file for analysis. All of the surface models were imported to MeshLab (Fig 1).[24] Any surrounding area around the specimen was systematically removed such that the final surface model STL only contained the specimen's surface.

A 3D-3D Geometric Comparison of iPhone Scanned Models Versus CT Models

Three-dimensional geometry of the surface models derived from iPhone and CT of the trochlea specimens

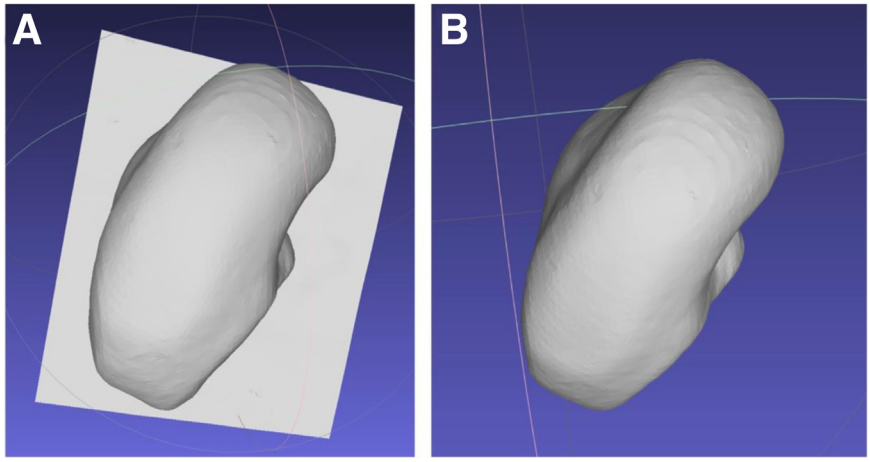

Fig 1. Postprocessing in MeshLab. (A) The surface model STL was imported from the iPhone scanning application into MeshLab for postprocessing to manually remove any surrounding area outside the specimen model. (B) The final surface model was then used for model analysis.

was compared by measuring surface-to-surface least distance distribution between a pair of overlapped models. Overlapping of the two 3D models was performed by 3D-3D registration using a validated volume merge method (accuracy, translation: 0.1 mm, rotation: 0.2°).[25] The surface-to-surface least distance between the two 3D models was calculated by a point-to-surface distance calculation algorithm to allow regional "inside/outside" evaluation of the model in addition to measuring an absolute distance between the two 3D models. In contrast, signed measurements provide positive or negative values of the surface-to-surface distance. Positive sign of the signed surface-to-surface distance (red color in Fig 1) represents that the iPhone model is larger than the CT model at the region. Negative sign of the signed surface-to-surface distance (blue color in Fig 2) represents that the iPhone model is smaller than the CT model at the region.[12]

Statistical Analysis

Statistical analysis was performed in Excel (Microsoft) and STATA (v13; STATAcorp). The data for the DFC were not normally distributed based on results using the Shapiro-Wilk test for normality. Therefore, nonparametric statistical analyses were employed, and results are reported as medians and interquartile ranges. A Kruskal-Wallis test with Dunn's post hoc test with Sidak correction was used to compare absolute and signed least mean square distances between the 3 tested specimen types (DFC, patella, and trochlea). Significance was set at $P < .05$.

Results

iPhone Scanning Application Feasibility and Model Selection

All 3 applications first underwent a qualitive model comparison by one of the senior authors (N.I.). A

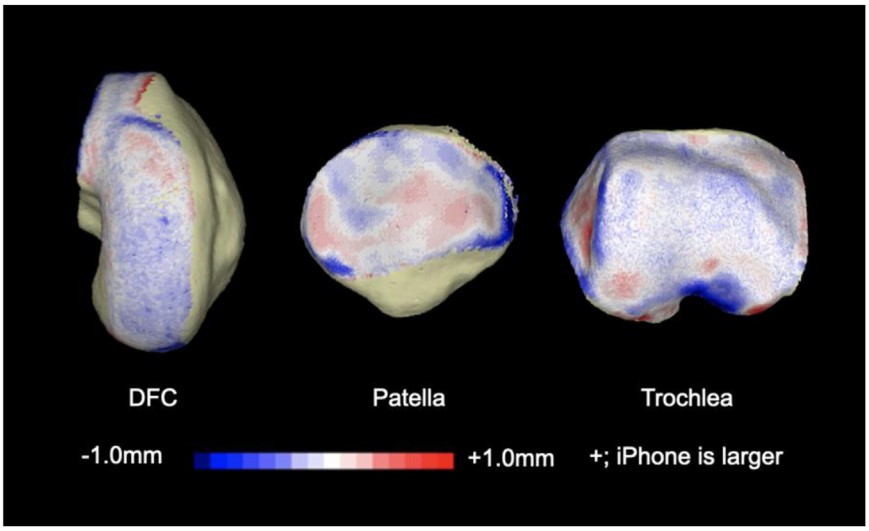

Fig 2. Representative images for each specimen type and the least mean distance comparison between iPhone scanning and computed tomography scan.

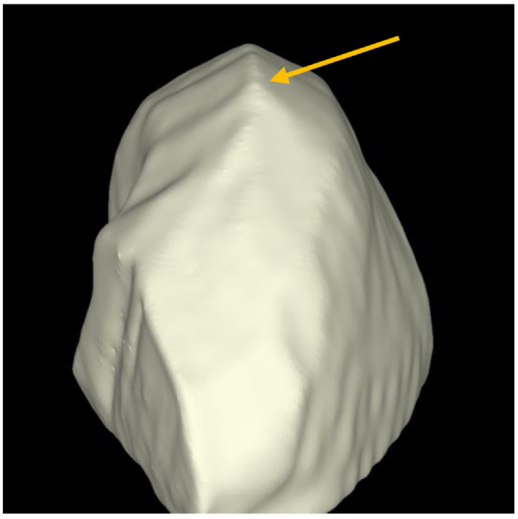

Fig 3. Qlone model of a distal condyle femur specimen demonstrating a pointed articular surface (yellow arrow). This artifact rendered the models unusable, and therefore, they were not quantitatively compared with the computed tomography models.

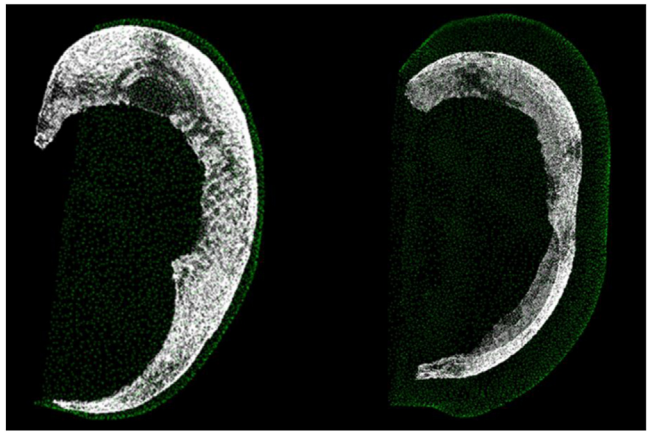

Fig 4. Two sagittal slices of Trnio models of a distal condyle femur specimen (green) compared with computed tomography (CT) (white) demonstrating inconsistencies in 3-dimensional (3D) model size compared with the CT scan. The 3D Trnio models were on average larger than the CT scans of the distal femoral condyle specimen.

qualitative evaluation of the Qlone models demonstrated that all of the specimens contained a peaked articular surface (Fig 3). Unfortunately, this artifact rendered the models unusable, and therefore, they were not quantitatively compared with the CT models. The Trnio models qualitatively appeared to demonstrate a similar surface topography to their correlating CT scans. However, during preliminary analysis, the Trnio models were found to be larger than the CT scan models (Fig 4). Preliminary surface topography analysis of the Trnio DFC specimen produced large signed (0.79 ± 0.34 mm, range: 0.18-1.53) and absolute least mean square differences (1.11 ± 0.27 mm, range: 0.63-1.65) quantitively supporting a model size difference compared with the CT scans of the DFC specimen. Previous studies have demonstrated significantly increased joint contact forces for OCA graft mismatches above 0.50 mm with significant changes in histologic architecture and cartilage thickening above 1.00 mm.[26-28] Given the average difference between the 3D Trnio models and CT scans being larger than these thresholds, the models were deemed unusable, and further quantitative analysis of the patella and trochlear specimens was not performed. Qualitatively, the Scandy models generated similar surface models to the CT scans, and no issues were encountered during analysis.

iPhone Scans Versus CT Scans

A total of 24 DFCs, 16 patellae, and 10 trochleae were included in the quantitative analysis comparing Scandy 3D models to CT models. There was a median absolute least mean square distance of 0.18 mm (interquartile range, 0.15-0.22 mm) (Table 1, Fig 5). Kruskal-Wallis testing demonstrated a significant difference in absolute least mean square distance based on location (P = .0038): the trochlea group had a significantly lower median absolute least mean square distance compared with the DFC group (P = .002). In evaluating the directionality of the difference between Scandy models and CT models (e.g., if Scandy models were larger or smaller compared with CTs), 100% of the trochleae demonstrated a negative signed least mean distance, as did 83% of the DFCs and 69% of the patellae (Figs 6-8). The patella specimen group was found to have a significantly higher signed least mean square distance compared to the DFC group (P = .030) and trochlea group (P = .029).

Discussion

This cadaveric analysis demonstrated several important findings with regard to the feasibility and accuracy of 3D iPhone scans in assessing chondral topography in the knee joint. First, this study demonstrated the

Table 1. Median and IQR Mean Square Distances (Signed and Absolute) for Each Specimen Type

Included Anatomy	Analysis Type	Median (IQR), mm
All specimens	Signed	−0.03 (−0.05 to 0.00)
	Absolute	0.18 (0.15 to 0.22)
DFC	Signed	−0.04 (−0.07 to 0.00)
	Absolute	0.19 (0.17 to 0.25)
Patella	Signed	−0.01 (−0.02 to 0.01)
	Absolute	0.17 (0.15 to 0.20)
Trochlea	Signed	−0.04 (−0.04 to −0.03)
	Absolute	0.14 (0.13 to 0.17)

DFC, distal femoral condyle; IQR, interquartile range.

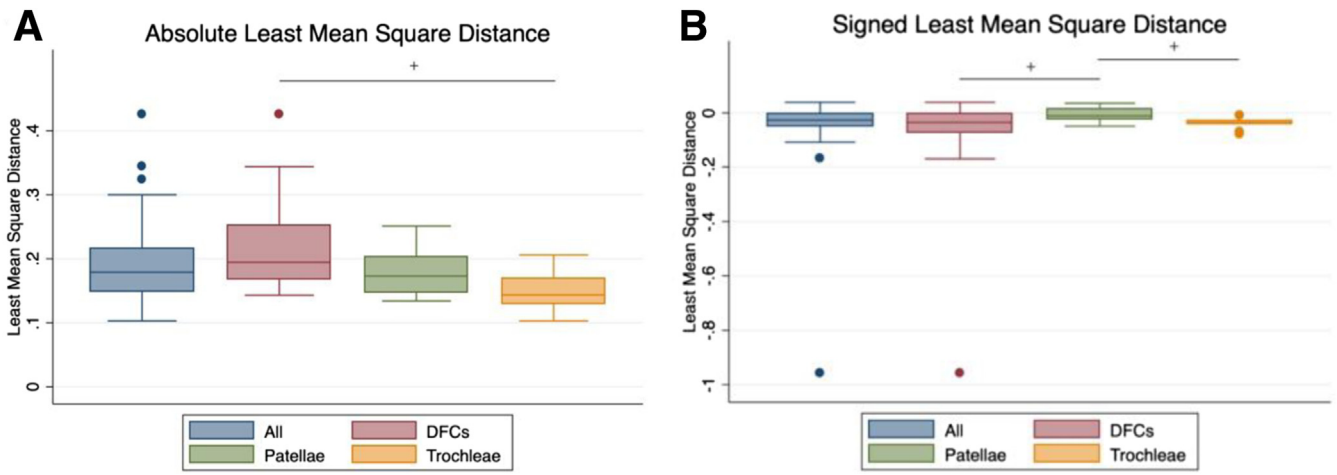

Fig 5. Histograms of the (A) absolute and (B) signed least mean square distances of all specimens and each category of specimen. $^{+}P < .05$. (DFC, distal femoral condyle.)

feasibility of scanning chondral surfaces with an iPhone-based application. Second, we identified Scandy as the preferred iPhone application for chondral topographical scanning. Third, this study found agreement between Scandy-obtained models and the clinical "gold standard" CT scanning when analyzing specimen chondral topography from 3 anatomic locations of the knee (patellae, distal femoral condyles, and trochleae).

In this study, the Scandy-produced models and CT-derived models had a median absolute least mean square distance of 0.18 mm. Previous studies have investigated imaging modalities such as MRI to CT and found absolute surface-to-surface mean differences between 0.37 and 0.83 mm depending on the MRI sequence.[12,29] Similarly, studies have compared CT and MRI with "ground-truth" surface models such as laser scanning, en face digital photography, and mechanical contact scanning and found absolute mean differences ranging from 0.15 to 0.75 mm for CT scans and 0.23 to 0.30 mm for MRI scans.[12,30,31] In addition, while the trochlea group had a significantly lower median absolute signed least mean square difference, all groups had a median of less than 0.20-mm difference between the iPhone model and CT model. This difference may be in part because the trochlea has a more complex shape and topography than a DFC. Together, our findings support the feasibility of iPhone-acquired chondral topography maps for different anatomic locations of the knee joint.

The 3D scanning with an iPhone could profoundly impact orthopaedic clinical practices, especially the OCA donor allograft harvesting process. Currently, commercial tissue banks do not have access to an MRI or a CT scan for their donor cadavers. Additionally, they are further constrained by the current Good Tissue Practice protocol that necessitates a 24-hour time frame from donor death in which they are required to harvest an OCA to limit contamination potential.[13,14] With current scanning technology and methods, this virtually inhibits the topography matching process. By providing commercial tissue banks with the ability to scan cadavers and create 3D models with an iPhone application, comparisons to preoperative patient imaging (CT or MRI) 3D models can be made and an optimal donor graft and harvest location can be found to minimize surface topography incongruity in patients. Furthermore, with the addition of AR applications, iPhone-based scanning could provide intraoperative guidance regarding optimal harvest locations on the donor specimen. This is especially useful if recipient chondral topography is observed to be different intraoperatively than what was indicated on preoperative imaging. For this purpose, iPhone scanning can be implemented without unnecessarily high risk to the sterile field as high-resolution scans can be acquired as far as 30 cm from object to iPhone, potentially even farther.[17] Moreover, this scanning technology could be adopted for other orthopaedic procedures such as an anatomic reconstruction of the anterior glenoid with distal tibial allograft in the setting of glenoid bone loss and shoulder instability. This procedure shares similarities to OCA transplantation in that anatomic osteochondral articular restoration of the anterior glenoid is required to avoid postoperative complications, such as graft resorption and osteolysis.[32,33] Simple iPhone scanning might aid in providing proper osteoarticular anatomic matching in this setting, which would allow the glenoid to maintain conformity with the humeral head through a full range of motion.[34,35]

Another finding in this study is that the median signed differences for all specimens (−0.03 mm), DFCs (−0.04 mm), trochleae (−0.03 mm), and patellae

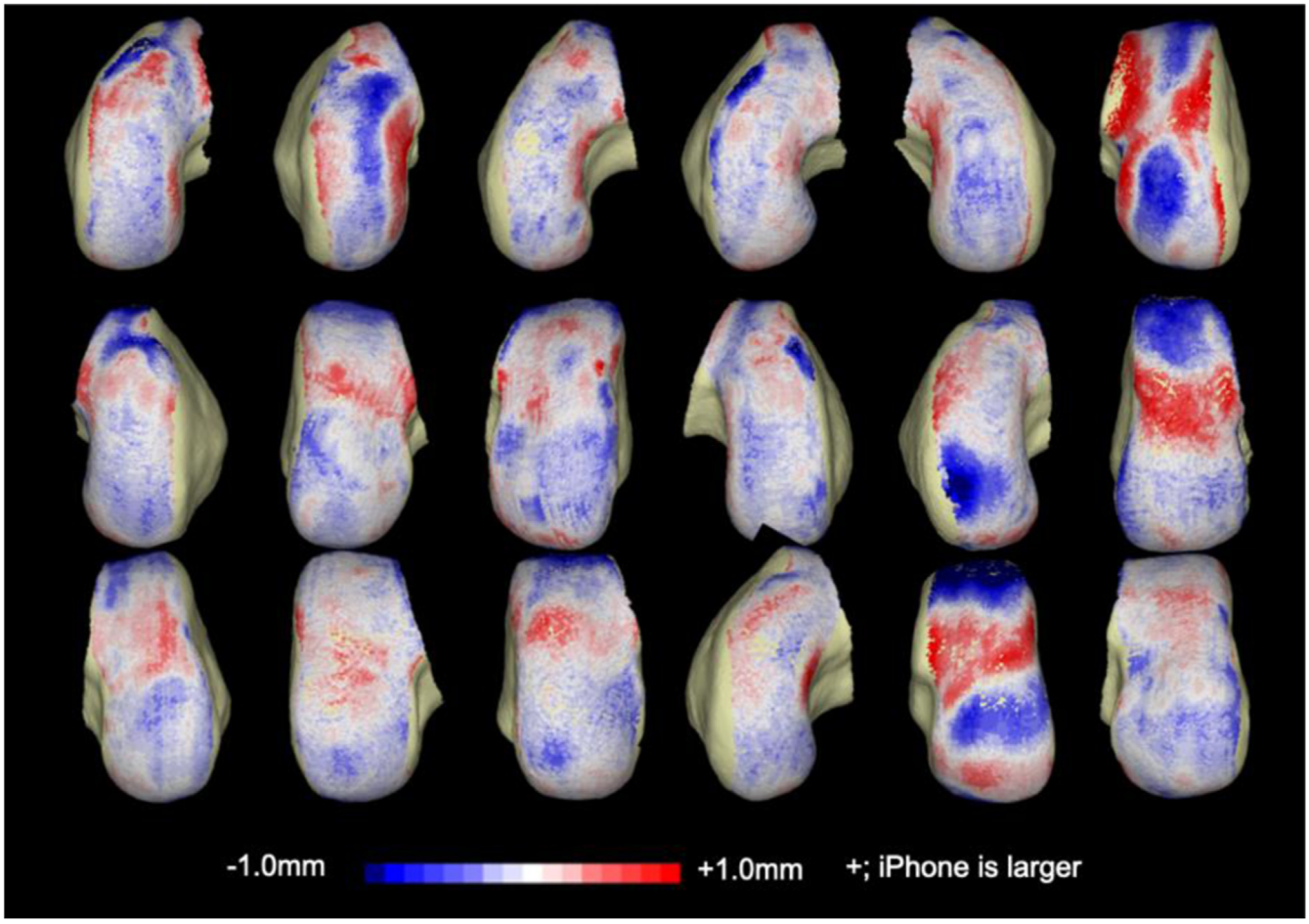

Fig 6. All included distal femoral condyles specimen models demonstrating signed least mean square distance between iPhone scanning and computed tomography scan.

(−0.01 mm) were lower relative to previously reported signed values for other imaging modality comparisons. Malloy et al.[12] examined signed surface-to-surface distances for MRI versus CT, MRI versus ground-trough laser scan, and CT versus laser scan, finding mean differences of 0.16 mm, 0.07 mm, and 0.27 mm, respectively (i.e., MRI models were the largest, followed by CT, with laser scans being the smallest). Similarly, in our study, we found that the iPhone models (generated from an infrared laser-based VCSEL technology) were smaller on average than CT-generated models. In fact, 100% of the trochleae, 83% of the DFCs, and 69% of the patellae specimens demonstrated a negative signed surface-to-surface distance when comparing iPhone versus CT. It currently remains unknown why laser-based models tend to be smaller on average than CT-based models and should be investigated in future studies.

Last, of the 3 iPhone applications examined for surface scanning in this study (Qlone, Trnio, and Scandy), only the Scandy application was able to create models adequate for analysis. This can likely be attributed to the different iPhone 3D camera and sensor technologies used for 3D scanning. Qlone and Trnio use the iPhone LiDAR sensor while Scandy uses the iPhone TrueDepth self-facing camera, which employs Apple's patented VCSEL technology.[17-19] LiDAR scanning calculates distances by emitting a light pulse and measuring the time difference in the returning light wave.[36] VCSEL technology, on the other hand, combines a traditional camera, infrared camera, proximity sensor, dot projector, and flood illuminator to emit and sense more than 30,000 points of infrared light to create a depth map and subsequent 3D model generated by machine learning algorithms.[20-23] Using VCSEL, the dots of the infrared pattern are more closely arranged than in LiDAR scanning. Thus, it can generate a much finer 3D mesh and is therefore well suited for scanning small objects (e.g., DFCs, patellae, and trochleae) while LiDAR is more appropriate in scanning large objects and rooms.[17] The results of our study reinforce these findings, as the Trnio and Qlone models utilizing LiDAR were inadequate for analysis compared with the successful models from Scandy 3D

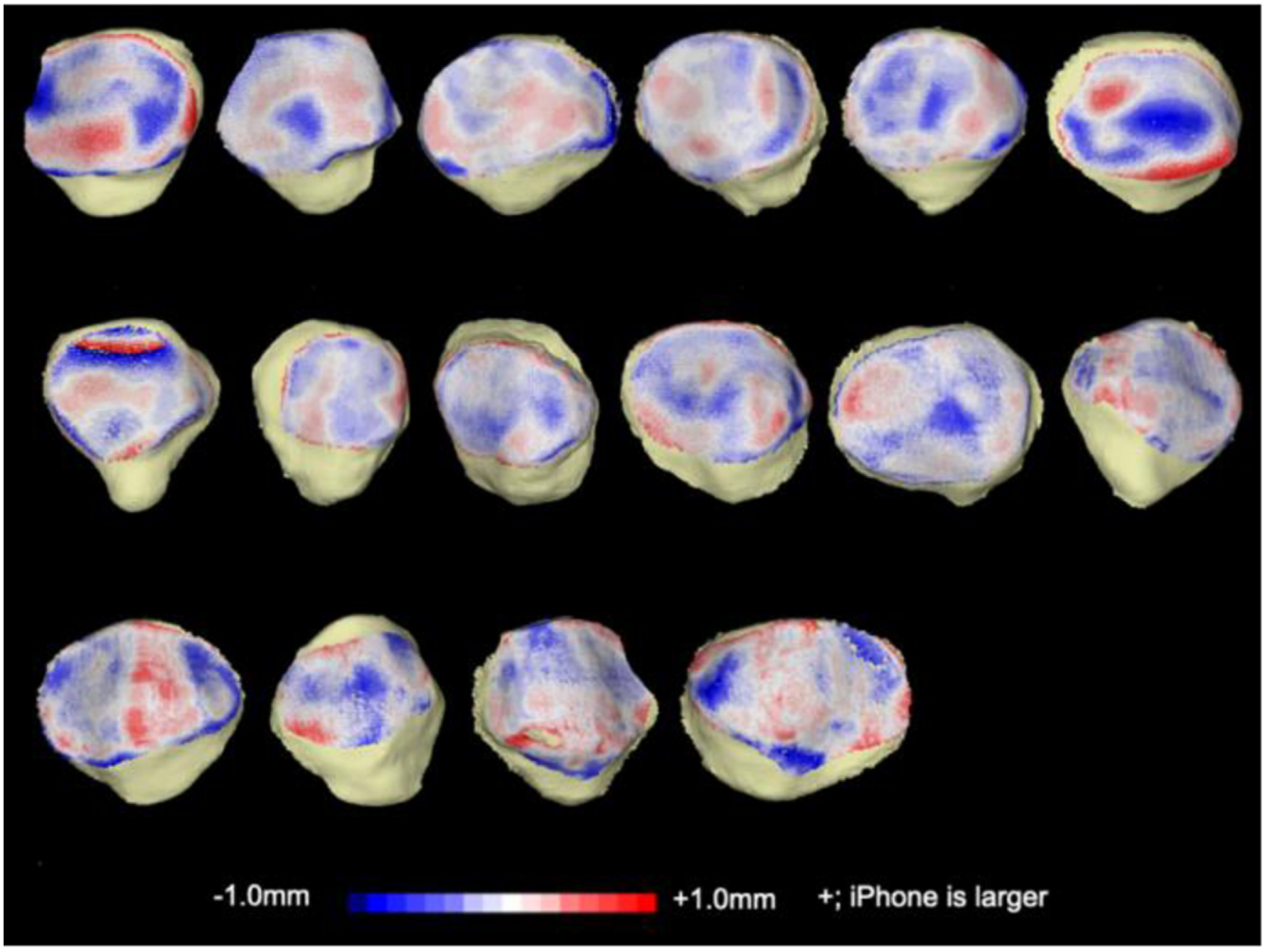

Fig 7. All included patella specimen models demonstrating signed least mean square distance between iPhone scanning and computed tomography scan.

scans utilizing VCSEL TrueDepth technology. This is further reflected in the primary uses of these underlying technologies in the iPhone as TrueDepth is used for facial authentication and recognition, while the LiDAR is intended for AR and plane detection for large rooms and open spaces.[17] Prior studies have investigated the accuracy of anatomic measurements using TrueDepth in other fields. For example, Amornvit and Sanohkan[23] investigated the accuracy of iPhone scanning models of 3D printed human phases using a TrueDepth technology-dependent application (Bellus3D). The authors reported that the iPhone demonstrated lower accuracy than the other model acquisition tools such as the EinScan Pro.[20-23] Similarly, Alfaro-Santafé et al.[22] reported on plantar foot scanning using TrueDepth technology (Scandy Pro 3D Scanner) and compared it with the Structure iSense scan, a previously validated scanning tool. The authors reported the iPhone scan provided excellent reliability (interclass coefficient > 0.9) in the X and Y planes and moderate reliability for arch height (interclass coefficient $= 0.74$). Surface scanning in orthopaedics is still in its infancy, and future studies will be needed to further explore its utility and validate its use.

Limitations

The current study is not without limitations. The 3D models generated from iPhone scanning were compared with models generated from the clinical "gold standard" CT scan. No comparisons were made to a "ground-truth" reference standard surface models such as laser scanning, en face digital photography, or mechanical contact scanning. A comparison to one of these reference standards in a future study would provide an additional layer of validation for iPhone scanning. In addition, this study selected anatomic samples only from the knee joint and specimen that had dysplasia, which would more likely reflect the patient's undergoing OCA procedures, but this may limit the generalizability of this study. The process of

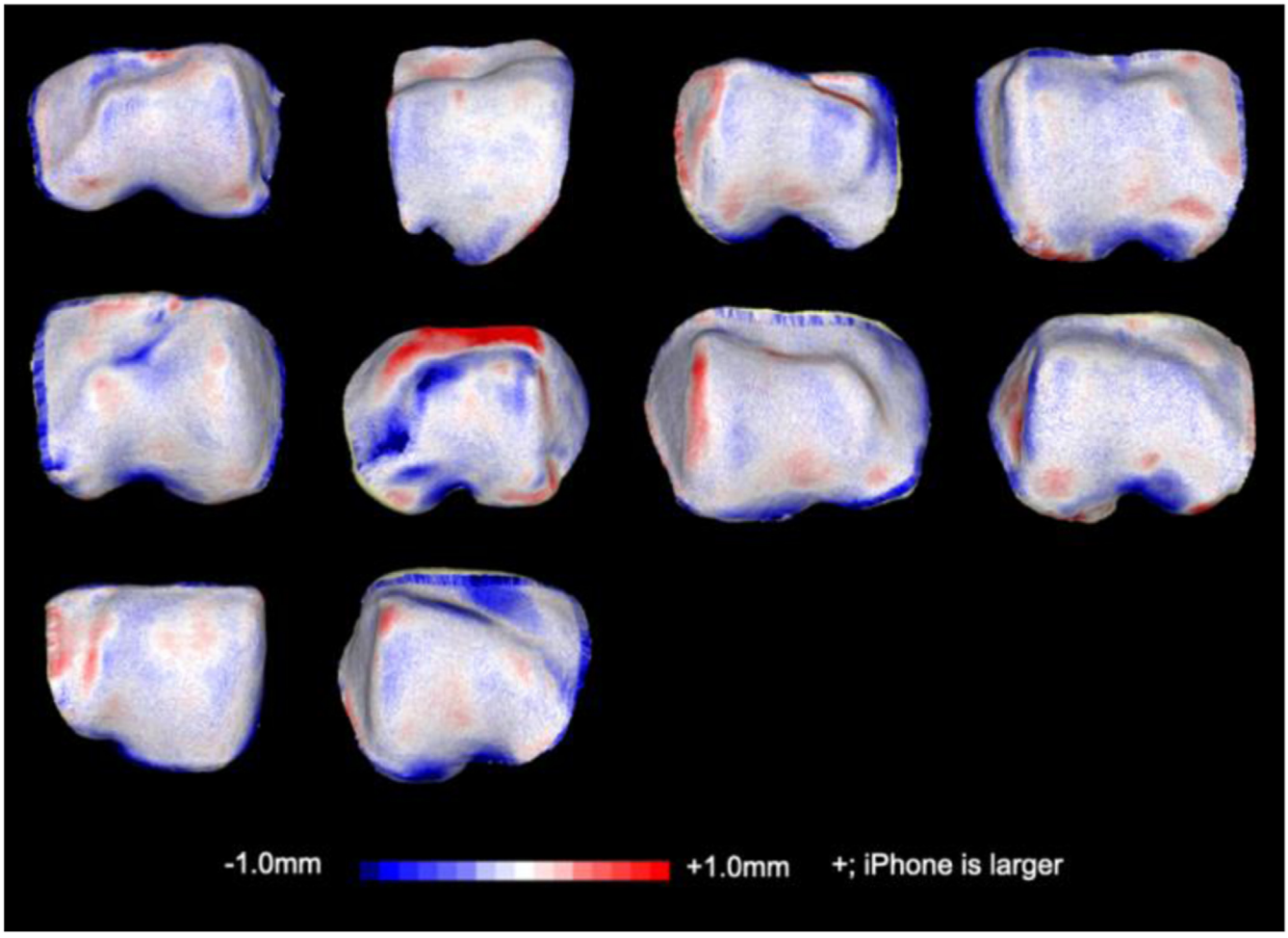

Fig 8. All included trochlea specimen models demonstrating signed least mean square distance between iPhone scanning and computed tomography scan.

creating an accurate, reproducible 3D model from an iPhone scan is also influenced by factors external to the device hardware and software as well. Scan accuracy can be affected by reflectance, shape, color, and surface texture of an object in addition to differences in ambient lighting.[17] The scanning distance between the object and iPhone and scanning strategy can also influence scan accuracy.[23,37,38] Each specimen was scanned based on scanning program instructions, and therefore, they were not scanned at the same distance, lighting, or position each time. There is a potential learning curve for the user that may affect the ability of 3D scans to be accurately captured and implemented into clinical practice. Furthermore, there was no intra- or interobserver reliability performed within this study.

Conclusions

In this study, we found minimal differences between a 3D iPhone scanning application and conventional CT scanning when analyzing surface topography.

Disclosures

The authors report the following potential conflicts of interest or sources of funding: M.H. has received personal fees from DJO-Enovis, Moximed, Vericel, and Elsevier outside the submitted work; has received royalties from Elsevier outside the submitted work; and is on the Editorial Board for the *Journal of Cartilage and Joint Preservation*. N.I. has received grants from the National Institutes of Health (NIAMS and NICHD) outside the submitted work. A.B.Y. has received personal fees from AlloSource, CONMED Linvatec, JRF Ortho, Olympus, Joint Restoration Foundation, and Medwest Associates outside the submitted work; has received grants from Arthrex and Vericel outside the submitted work; has received nonfinancial support from Organogenesis, Patient IQ, Smith & Nephew, and Sparta Biomedical outside the submitted work; and has stocks with Patient IQ. All other authors (H.P.H., K.C., M.M.A., W.M.C.) declare that they have no known competing financial interests or personal relationships that could have appeared to influence the work

reported in this paper. Full ICMJE author disclosure forms are available for this article online, as supplementary material.

References

1. Årøen A, Løken S, Heir S, et al. Articular cartilage lesions in 993 consecutive knee arthroscopies. *Am J Sports Med* 2004;32:211-215.
2. Curl WW, Krome J, Gordon ES, Rushing J, Smith BP, Poehling GG. Cartilage injuries: A review of 31,516 knee arthroscopies. *Arthroscopy* 1997;13:456-460.
3. Jamali AA, Emmerson BC, Chung C, Convery FR, Bugbee WD. Fresh osteochondral allografts: Results in the patellofemoral joint. *Clin Orthop Relat Res* 2005;437:176-185.
4. Emmerson BC, Görtz S, Jamali AA, Chung C, Amiel D, Bugbee WD. Fresh osteochondral allografting in the treatment of osteochondritis dissecans of the femoral condyle. *Am J Sports Med* 2007;35:907-914.
5. Rue JPH, Yanke AB, Busam ML, McNickle AG, Cole BJ. Prospective evaluation of concurrent meniscus transplantation and articular cartilage repair: Minimum 2-year follow-up. *Am J Sports Med* 2008;36:1770-1778.
6. Stone KR, Adelson WS, Pelsis JR, Walgenbach AW, Turek TJ. Long-term survival of concurrent meniscus allograft transplantation and repair of the articular cartilage. *J Bone Joint Surg Br* 2010;92:941-948.
7. Meyers MH, Akeson W, Convery FR. Resurfacing of the knee with fresh osteochondral allograft. *J Bone Joint Surg Am* 1989;71:704-713.
8. Familiari F, Cinque ME, Chahla J, et al. Clinical outcomes and failure rates of osteochondral allograft transplantation in the knee: A systematic review. *Am J Sports Med* 2018;46:3541-3549.
9. Assenmacher AT, Pareek A, Reardon PJ, Macalena JA, Stuart MJ, Krych AJ. Long-term outcomes after osteochondral allograft: A systematic review at long-term follow-up of 12.3 years. *Arthroscopy* 2016;32:2160-2168.
10. Thaunat M, Couchon S, Lunn J, Charrois O, Fallet L, Beaufils P. Cartilage thickness matching of selected donor and recipient sites for osteochondral autografting of the medial femoral condyle. *Knee Surg Sports Traumatol Arthrosc* 2007;15:381-386.
11. Nakagawa Y, Suzuki T, Kuroki H, Kobayashi M, Okamoto Y, Nakamura T. The effect of surface incongruity of grafted plugs in osteochondral grafting: A report of five cases. *Knee Surg Sports Traumatol Arthrosc* 2007;15:591-596.
12. Malloy P, Gasienica J, Dawe R, et al. 1.5 T magnetic resonance imaging generates accurate 3D proximal femoral models: Surgical planning implications for femoroacetabular impingement. *J Orthop Res* 2020;38:2050-2056.
13. Görtz S, Bugbee W. Fresh osteochondral allografts—graft processing and clinical applications. *J Knee Surg* 2006;19:231-240.
14. Pennock A, Wagner F, Robertson C, Harwood F, Bugbee W, Amiel D. Prolonged storage of osteochondral allografts—does the addition of fetal bovine serum improve chondrocyte viability? *J Knee Surg* 2006;19:265-272.
15. Casari FA, Navab N, Hruby LA, et al. Augmented reality in orthopedic surgery is emerging from proof of concept towards clinical studies: A literature review explaining the technology and current state of the art. *Curr Rev Musculoskelet Med* 2021;14:192-203.
16. Laverdière C, Corban J, Khoury J, et al. Augmented reality in orthopaedics: A systematic review and a window on future possibilities. *Bone Joint J Br* 2019;101:1479-1488.
17. Vogt M, Rips A, Emmelmann C. Comparison of iPad Pro®'s LiDAR and TrueDepth capabilities with an industrial 3D scanning solution. *Technologies* 2021;9:25.
18. Mune CD. Supporting 3D: Potential practices for the creation and preservation of 3D/VR in libraries. *Public Serv Q* 2022;18:209-217.
19. Dzelzkalēja L, Knēts JK, Rozenovskis N, Sīlītis A. Intelligent systems and applications. *Proceedings of the 2021 Intelligent Systems Conference (IntelliSys)*, 2 Berlin, Germany: Springer International Publishing, 2021;34-50;2, 2021. Lecture Notes in Networks and Systems.
20. Carey N, Werfel J, Nagpal R. Fast, accurate, small-scale 3D scene capture using a low-cost depth sensor. *2017 IEEE Winter Conf Appl Comput Vis Wacv* 2017;2017:1268-1276.
21. Olade I, Liang HN, Fleming C. A review of multimodal facial biometric authentication methods in mobile devices and their application in head mounted displays In: *2018 Institute of Electrical and Electronics Engineers (IEEE) SmartWorld, Ubiquitous Intelligence & Computing, Advanced & Trusted Computing, Scalable Computing & Communications, Cloud & Big Data Computing, Internet of People and Smart City Innovation (SmartWorld/SCALCOM/UIC/ATC/CBDCom/IOP/SCI)*. Piscataway, NJ: Institute of Electrical and Electronics Engineers (IEEE), 2018;1997-2004.
22. Alfaro-Santafé J, Gómez-Bernal A, Lanuza-Cerzócimo C, Alfaro-Santafé JV, Pérez-Morcillo A, Almenar-Arasanz AJ. Three-axis measurements with a novel system for 3D plantar foot scanning: iPhone X. *Footwear Sci* 2020;12:123-131.
23. Amornvit P, Sanohkan S. The accuracy of digital face scans obtained from 3D scanners: An in vitro study. *Int J Environ Res Public Health* 2019;16:5061.
24. Cignoni P, Callieri M, Corsini M, Dellepiane M, Ganovelli F, Ranzuglia G. MeshLab: An open-source mesh processing tool. In: Scarano V, Chiara RD, Erra U, eds. *Eurographics Italian Chapter Conference*. Pisa, Italy: The Eurographics Association, 2008;129-136.
25. Ochia RS, Inoue N, Renner SM, et al. Three-dimensional in vivo measurement of lumbar spine segmental motion. *Spine* 2006;31:2073-2078.
26. Huang FS, Simonian PT, Norman AG, Clark JM. Effects of small incongruities in a sheep model of osteochondral autografting. *Am J Sports Med* 2004;32:1842-1848.
27. Du PZ, Markolf KL, Boguszewski DV, et al. Effects of proud large osteochondral plugs on contact forces and knee kinematics: A robotic study. *Am J Sports Med* 2018;46:2122-2127.
28. Koh JL, Wirsing K, Lautenschlager E, Zhang LO. The effect of graft height mismatch on contact pressure following osteochondral grafting: A biomechanical study. *Am J Sports Med* 2004;32:317-320.

29. Neubert A, Wilson KJ, Engstrom C, et al. Comparison of 3D bone models of the knee joint derived from CT and 3T MR imaging. *Eur J Radiol* 2017;93:178-184.
30. Rathnayaka K, Momot KI, Noser H, et al. Quantification of the accuracy of MRI generated 3D models of long bones compared to CT generated 3D models. *Med Eng Phys* 2012;34:357-363.
31. Gyftopoulos S, Yemin A, Mulholland T, et al. 3DMR osseous reconstructions of the shoulder using a gradient-echo based two-point Dixon reconstruction: A feasibility study. *Skeletal Radiol* 2013;42:347-352.
32. Zhu YM, Jiang CY, Lu Y, Li FL, Wu G. Coracoid bone graft resorption after Latarjet procedure is underestimated: A new classification system and a clinical review with computed tomography evaluation. *J Shoulder Elbow Surg* 2015;24:1782-1788.
33. Boehm E, Minkus M, Moroder P, Scheibel M. Massive graft resorption after iliac crest allograft reconstruction for glenoid bone loss in recurrent anterior shoulder instability. *Arch Orthop Trauma Surg* 2020;140:895-903.
34. Decker MM, Strohmeyer GC, Wood JP, et al. Distal tibia allograft for glenohumeral instability: Does radius of curvature match? *J Shoulder Elbow Surg* 2016;25:1542-1548.
35. Provencher MT, Ghodadra N, LeClere L, Solomon DJ, Romeo AA. Anatomic osteochondral glenoid reconstruction for recurrent glenohumeral instability with glenoid deficiency using a distal tibia allograft. *Arthroscopy* 2009;25:446-452.
36. Schuon S, Theobalt C, Davis J, Thrun S. High-quality scanning using time-of-flight depth superresolution In: *2008 IEEE Comput Soc Conf Comput Vis Pattern Recognit Work* 2008;1-7.
37. Gerbino S, Giudice DMD, Staiano G, Lanzotti A, Martorelli M. On the influence of scanning factors on the laser scanner-based 3D inspection process. *Int J Adv Manuf Technol* 2016;84(9-12):1787-1799.
38. Ameen W, Al-Ahmari A, Mian SH. Evaluation of hand-held scanners for automotive applications. *Appl Sci* 2018;8:217.